Vicinal Si(100) surfaces under external strain

K. Cho, J. D. Joannopoulos, and A. Nihat Berker
Department of Physics, Massachusetts Institute of Technology, Cambridge, Massachusetts 02139
(Received 13 April 1995; revised manuscript received 11 September 1995)

The phase diagram of vicinal Si(100) surfaces is calculated as a function of misorientation angle, temperature, and applied external strain. It is shown that a change of the applied external strain can lead to a phase transition between the single-layer step surface phase and the double-layer step surface phase. The effect of temperature is shown to be negligible up to 300 K. The order parameter of the surface phase transition is also calculated to make contact with experimental measurements.

I. INTRODUCTION

When a Si crystal is cut by a plane slightly misoriented toward the (011) direction from the (100) surface, the crystal surface accommodates the misorientation by generating low-energy steps on the Si(100) surface. On a vicinal Si(100) surface there are two types of low-energy steps observed experimentally, i.e., single-layer (SL) steps and double-layer steps. There are two different single-layer steps (SA and SB), depending on the orientations of the dimers on the terraces separated by the step, as shown in Fig. 1(a). There are also two different double-layer steps (DA and DB), but of these essentially only DB steps [Fig. 1(b)] are observed experimentally. A simple tight-binding calculation of the energies of the steps, neglecting the interaction between steps, indicates that the DB step has the lowest formation energy.[1] The neglect of interactions is not a serious problem for double-layer steps. Single-layer steps, however, interact with each other through the relaxations of the strain on the alternating (2×1) and (1×2) terraces, and this interaction can significantly lower the surface energy of the single-layer step surface. Alerhand *et al.*[2] showed that for small misorientation angles ($\theta<\theta_c$) the interaction energy is large enough to make the SL step surface the ground-state geometry at zero temperature. Furthermore, at a finite temperature steps are not straight but fluctuating, as illustrated in Fig. 1 for SB and DB steps, and the fluctuations lower the step free energies. The SB step has the lowest energy for kink formation, and consequently shows the largest fluctuations in the experimental observations. The large fluctuation of the SB step at finite temperature lowers the surface free energy of the SL step surface relative to that of the DB step surface so that the critical angle θ_c increases as a function of temperature.[2] Alerhand *et al.* showed that the temperature versus misorientation-angle phase digram has two phases, the DB step surface and the SL step surface, divided by a first-order phase transition line.[2]

Subsequently, it was shown that the higher-order terms (dipole terms) in the step interactions lead to phases of mixed step surfaces between the DB step surface phase and SL step surface phase.[3,4] Furthermore, at high temperature ($T>500$ K) the step fluctuations are large enough that different surface phases (SL, mixed, and DB step surfaces) become indistinguishable.[4]

In this paper, we introduce the external strain as a controllable parameter and calculate a more general phase diagram of the vicinal Si(100) surface in the three-dimensional parameter space: the misorientation angle θ, the temperature T, and the applied external strain ϵ.

II. CALCULATIONS

The free energy of a vicinal surface of miscut angle θ is determined from three terms: the step energy, the renormalization of the step energy due to the fluctuation of the steps at finite temperature, and the step interaction energy. If λ_{SA} and λ_{SB} are the formation energies per unit length [$2a$, where a is the (1×1) surface unit length] for the SA step and the SB step, the step energy per unit area $(2a)^2$ for the SL step surface is

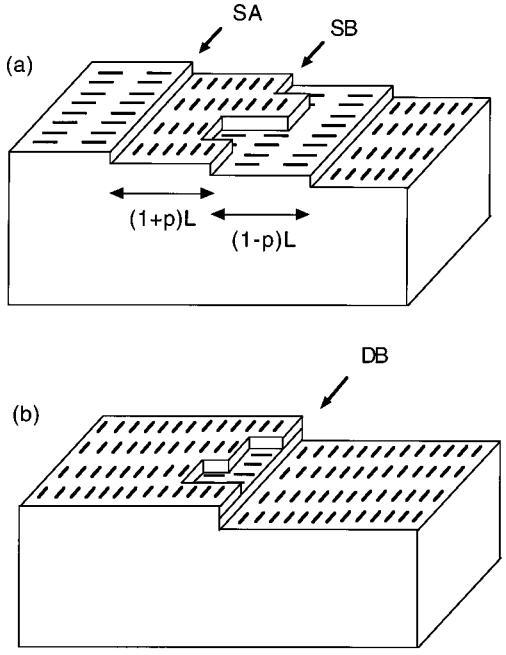

FIG. 1. Schematic representation of (a) the single-layer and (b) the double-layer structures of a vicinal Si(100) surface. The thermal fluctuations of the SB and DB step edges show only the rebonded step edges, and the unit length of the fluctuation is $2a$, where a is the (1×1) surface unit length.

$$E_{\text{step}}(L)=\frac{\lambda_{\text{SA}}+\lambda_{\text{SB}}}{2L}, \tag{2.1}$$

where L (in the unit of $2a$) is related to θ by $\tan(\theta)=1.36$ Å $/L$ (1.36 Å is the height of a single layer step). Similarly, if λ_{DB} is the formation energy per unit length $(2a)$ for the DB step, the DL step energy per unit area is $\lambda_{\text{DB}}/2L$.

The effect of thermal fluctuations of steps is calculated using the Hamiltonian of a one-dimensional solid-on-solid (SOS) model for the SB step and the DB step.[2] The thermal fluctuation of the SA step is not included because it has a much higher kink formation energy than the SB and DB steps. The free energy per unit length of the SB step at a temperature T is then

$$\lambda_{\text{SB}}-\frac{k_BT}{N}\ln Z_{H(\text{SB})}, \tag{2.2}$$

where $Z_{H(\text{SB})}$ is the partition function of the one-dimensional SOS model for the SB step, and N is the number of step units in $H(\text{SB})$. $H(\text{SB})$ is the one-dimensional SOS model Hamiltonian for the SB step,

$$H(\text{SB})=\sum_{i=1}^{N}\{\lambda_{\perp}|l_{i+1}-l_i|+2\epsilon_c(1-\delta_{l_{i+1},l_i}) +\kappa(\theta,\epsilon)|l_i-l(\theta,\epsilon)|^2\}, \tag{2.3}$$

where l_i is the terrace width at position i along the step, $\lambda_{\perp}$ is the SA step kink formation energy, ϵ_c is the corner energy of the kink, and $\kappa(\theta,\epsilon)$ is the stiffness coefficient of the confinement potential obtained from the second-order coefficient for a change of the relative terrace width [i.e., the change of p in Fig. 1(a)] from the equilibrium value at the given θ and ϵ, $l(\theta,\epsilon)$.[5] Similarly, the free energy of the DB step is

$$\lambda_{\text{DB}}-\frac{k_BT}{N}\ln Z_{H(\text{DB})}, \tag{2.4}$$

where $H(\text{DB})$ is the one-dimensional SOS model Hamiltonian for the DB step. $H(\text{DB})$ describes the fluctuation of the DB step in which both the SA and SB steps are generated as illustrated in Fig. 1(b), and

$$H(\text{DB})=\sum_{i=1}^{N}\{\lambda_{\perp}|l_{i+1}-l_i|+2\epsilon_c(1-\delta_{l_{i+1},l_i}) +\lambda_{\parallel}(1-\delta_{l_i,2L})\}, \tag{2.5}$$

where $\lambda_{\parallel}$ is the energy of breaking the DB step into a pair of SA and SB steps. The calculated free energies for the SB step and the DB step are shown in Fig. 2. The SB step free energy is negligibly small up to 300 K, and the DB step free energy is negligibly small up to 500 K. These behaviors of the step free energies are consistent with the experimental observations that only SB steps show significant thermal fluctuations in $300\ \text{K}<T<500$ K, and consequently the SOS model Hamiltonian for the DB step is good enough to describe this essential aspect of the DB step thermal fluctuations. Around 500 K the SB step fluctuation is significant enough to disorder the surface so that for all practical purposes the DB step fluctuations are negligible.[6]

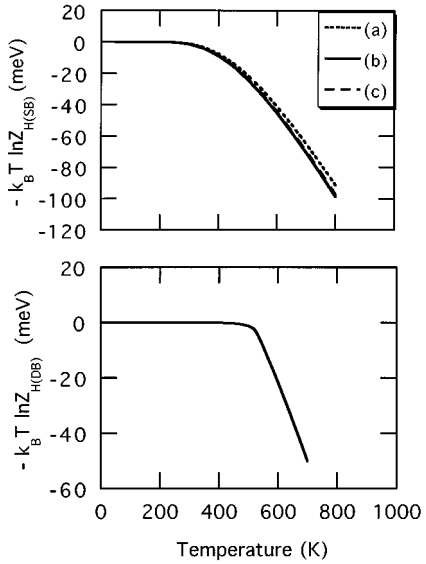

FIG. 2. Free energies of the SB step (top panel) and the DB step (bottom panel) as a function of temperature. For the SB step $\theta=0.6°$ and (a) $\epsilon=-0.1\%$, (b) $\epsilon=0\%$, and (c) $\epsilon=0.05\%$ are used for κ.

Finally, the strain energy has two terms for the SL step surface: the strain relaxation energy and the strain energy of the applied external strain. The lowest-order strain relaxation energy is

$$E^{(1)}_{\text{strain}}(L)=-L^{-1}\lambda_{\sigma}\ln\left(\frac{L}{\pi}\cos\frac{\pi p}{2}\right), \tag{2.6}$$

where λ_{σ} is determined by surface stress anisotropy, and p is the fraction of increased domain due to an applied external strain [i.e., the alternating domains have unequal widths $(1+p)L$ and $(1-p)L$ as illustrated in Fig. 1(a)]. The higher-order terms from the dipole interactions are

$$E^{(2)}_{\text{strain}}(L)=\frac{\lambda_d}{(2L)^3}-\frac{\sqrt{3\lambda_{\sigma}\lambda_d}}{2L^2}\tan\frac{\pi p}{2}, \tag{2.7}$$

where λ_d is determined from the dipole moments of the SL steps. The external strain energy is

$$\begin{aligned}E^{\text{ext}}_{\text{strain}}(L,\epsilon)&=(2L)^{-1}[(1+p)L\sigma_{\perp}\epsilon+(1-p)L\sigma_{\parallel}\epsilon]\\&=1/2\epsilon p(\sigma_{\perp}-\sigma_{\parallel})+1/2\epsilon(\sigma_{\perp}+\sigma_{\parallel})\\&=1/2\epsilon p(\sigma_{\perp}-\sigma_{\parallel}),\end{aligned} \tag{2.8}$$

where $\sigma_{\parallel}$ is the stress tensor component along the dimer direction and $\sigma_{\perp}$ is the component perpendicular to the dimer direction, and $\sigma_{\perp}=-\sigma_{\parallel}$ is used. On the other hand there is no strain relaxation for the DB step surface. The external strain energy for the DB step surface is $\epsilon\sigma_{\perp}$.[7]

Putting the energy terms together, the free energies per unit area for the SL step surface and DB step surface are given by

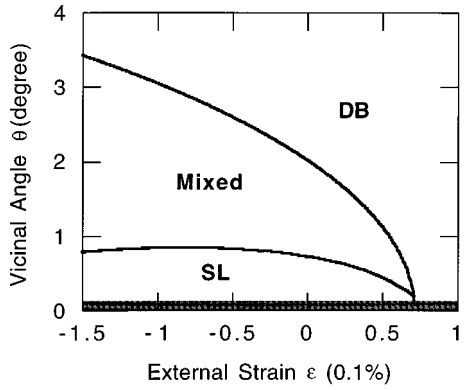

FIG. 3. Phase diagram on the plane of the external strain and the vicinal angle. Three phases are indicated as DB, mixed, and SL: the DB double-layer step surface, the mixed-layer surface phases, and the single-layer surface. The gray region for small vicinal angles represents the phase of spontaneous stress domains which are not included in the calculations.

$$F_{\mathrm{SL}}(L,T,\epsilon)=\frac{\lambda_{\mathrm{SA}}+\lambda_{\mathrm{SB}}-\frac{k_BT}{N}\ln Z_{H(\mathrm{SB})}}{2L} -L^{-1}\lambda_\sigma \ln\left(\frac{L}{\pi}\cos\frac{\pi p}{2}\right)+\frac{\lambda_d}{(2L)^3} -\frac{\sqrt{3\lambda_\sigma\lambda_d}}{2L^2}\tan\frac{\pi p}{2}+1/2\epsilon p(\sigma_\perp-\sigma_\parallel), \tag{2.9}$$

$$F_{\mathrm{DB}}(L,T,\epsilon)=\frac{\lambda_{\mathrm{DB}}-\frac{k_BT}{N}\ln Z_{H(\mathrm{DB})}}{2L}+\epsilon\sigma_\perp . \tag{2.10}$$

Here the fraction p in the F_{SL} is determined by minimizing the strain energy with fixed L. The energy parameters used for the free energies are the same as in Ref. 8.

III. PHASE DIAGRAM

The phase diagram in the three-dimensional parameter space (θ, T, and ϵ) is determined as follows. For a given T and ϵ the surface free energies F_{SL} and F_{DB} are calculated as a function of θ. By taking a cotangent line to the $F_{\mathrm{SL}}(\theta)$ and $F_{\mathrm{DB}}(\theta)$ curves, the boundaries of the mixed step surface phase are determined as $\theta_{c1}(T,\epsilon)$ and $\theta_{c2}(T,\epsilon)$ following the cotangent construction approach introduced in Refs. 3 and 4. The cotangent construction specifies the range of stability for the SL and DB phases, and the mixed phases are stable between these two phases. The phase transition from SL phase into an infinite sequence of the mixed step surface phases is basically driven by an infinite sum of infinite range step-step interactions.

Figure 3 shows a projection of the phase diagram on the two-dimensional parameter space (ϵ and θ) at $T=0$. The SL step surface and the mixed step surface is separated by the line of critical angle $\theta_{c1}(T=0,\epsilon)$, and the DB step surface and the mixed step surface is separated by the line of critical angle $\theta_{c2}(T=0,\epsilon)$. The critical angles increase for negative external strain, and the mixed step surface phase is stable over a wide range of vicinal angle. On the other hand, for positive external strain the critical angles decrease and become zero at $\epsilon=0.07\%$. For an external strain larger than 0.07% only the DB step surface is a stable phase. However, one should note that at a small vicinal angle ($\theta<\theta_{\mathrm{domain}}=0.08°-0.25°$) the terraces are large enough to form spontaneous stress domains, and a different type of surface phase becomes stable, as indicated in Fig. 3.[7]

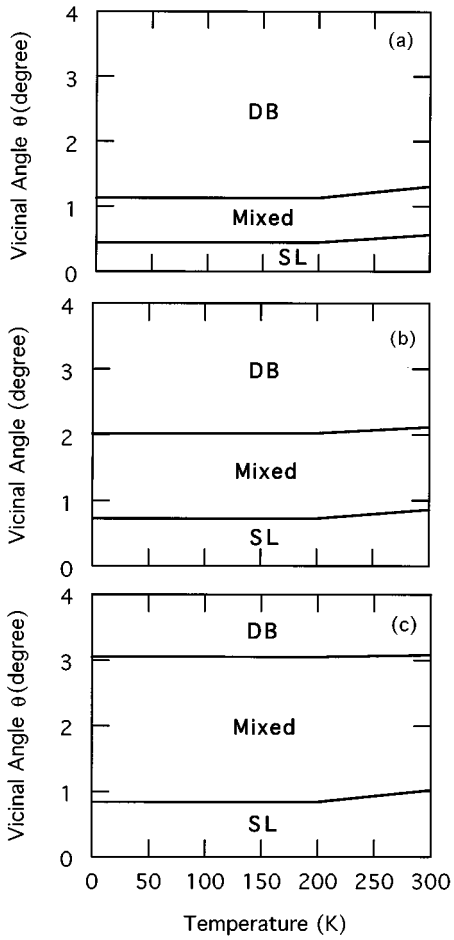

FIG. 4. Phase diagram on the plane of the temperature and the vicinal angle at (a) $\epsilon=0.05\%$, (b) $\epsilon=0\%$, and (c) $\epsilon=-0.1\%$.

Figure 4 shows three projections of the phase diagram on the two-dimensional parameter space (T and θ) at $\epsilon=0.05\%$, 0%, and -0.1%. The three surface phases are separated by two lines of critical angles $\theta_{c1}(T,\epsilon)$ and $\theta_{c2}(T,\epsilon)$ at fixed ϵ. These critical angles show very small changes as the temperature increases from 0 to 300 K, and this temperature dependence is consistent with the behavior of the step free energies shown in Fig. 2. For $\epsilon=0\%$ this phase diagram reproduces the results of Pehlke and Tersoff.[4] This small temperature dependence of $\theta_{c1}(T,\epsilon)$ and $\theta_{c2}(T,\epsilon)$ for $T<300$ K immediately leads to the fact that the ϵ-θ phase digram at any $T<300$ K is practically identical to Fig. 3.

As the temperature increases further, the SB step free energy decreases rapidly (Fig. 2) so that the step fluctuation becomes large. For this high temperature ($T>300$ K) the

difference between a DB step and a pair of the SB step and the SA step gradually disappears as the temperature increases, and consequently the three phases (DB, mixed, and SL step surfaces) become indistinguishable, presumably via another disordering phase transition.[6]

We note that for $T<300$ K the diffusion of surface atoms is so slow that the surface steps will not move under the applied external strain to reach a global minimum energy geometry. Consequently, one needs to anneal the surface at higher temperature in the presence of an external strain to obtain the ϵ-θ phase digram of Fig. 3. However, if the freeze-in temperature in the annealing process is higher than 300 K, then the phase diagram in Fig. 3 is not directly accessible in experiments. Furthermore, if the freeze-in temperature is higher than 500 K, then experiments cannot observe any phase transitions. The scanning tunneling microscopy image of the vicinal surface (0.3° miscut) under external strain in Ref. 9 shows a clear SL surface phase. This experiment indicates either that the freeze-in temperature is lower than 500 K or that a freeze-in temperature higher than 500 K does not significantly influence the SL step surface structure at the 0.3° miscut angle. Therefore, in practice the phase diagram in Fig. 3 can at least serve as a guide to experiments showing that a set parameters ϵ-θ will lead to a certain surface step structure after annealing.

IV. ORDER PARAMETER

The order parameter of the surface phase is defined to be the fraction of the domain (p) as illustrated in Fig. 1. For the DB step surface $p=1$, and for the mixed step and the SL step surfaces $-1<p<1$ at zero temperature. Since the order parameter measures the relative fraction of two types of surface terraces, and it can be measured directly in a low-energy electron-diffraction (LEED) experiment, we predict the following behavior of the order parameter as a function of the vicinal angle and the external strain. Note that the temperature effect is not important because the step fluctuations do not change the average value of p which is measured in experiments.

The top panel of Fig. 5 shows the order parameter as a function of the vicinal angle at fixed external strain. The general trend is that the order parameter increases as the vicinal angle increases for both positive and negative external strain. A positive strain increases the order parameter, but a negative strain decreases the order parameter. The small-angle behavior of the order parameter is not accurate because a different surface phase becomes stable for $\theta<\theta_{\text{domain}}$ as noted before.[7]

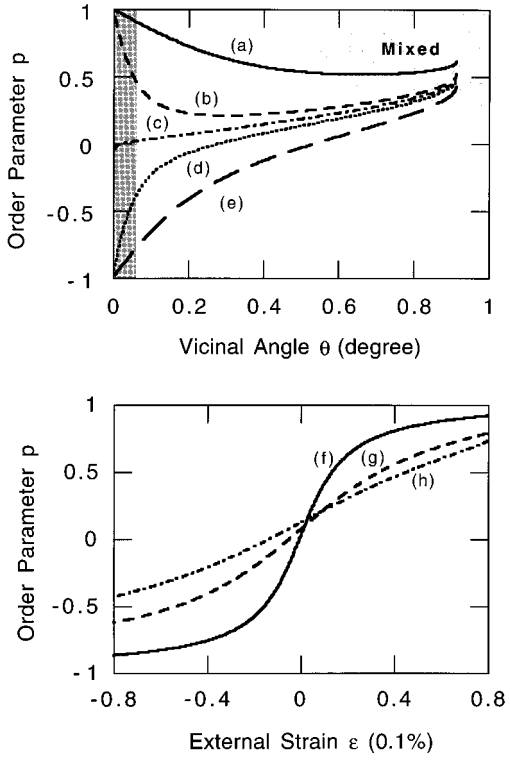

FIG. 5. Top panel shows a plot of order parameter p as a function of the vicinal angle at the external strain (a) 0.05%, (b) 0.01%, (c) 0%, (d) -0.01%, and (e) -0.05%. The order parameter is calculated for the SL phase and is not applicable to the dark gray region corresponding to the phase of spontaneous stress domains and the light gray region corresponding to the mixed phases. Bottom panel shows a plot of order parameter as a function of the external strain at vicinal angles (f) 0.1°, (g) 0.3°, and (h) 0.5°.

The bottom panel of Fig. 5 shows the order parameter as a function of the external strain at three vicinal angles (0.1°, 0.3°, and 0.5°). These results agree quantitatively with the experimental measurement of the order parameter p by Webb *et al.*[9] The result in Fig. 6 of Ref. 9 shows a very good quantitative agreement with the theoretical predictions in the bottom panel of Fig. 5. More specifically, the experiment has found $p=0.6$ for $\theta=0.3°$ and $\epsilon=0.04\%$ in an excellent agreement with the theoretical value $p=0.59$.

[1] D. J. Chadi, Phys. Rev. Lett. **59**, 1691 (1987).

[2] O. L. Alerhand, A. N. Berker, J. D. Joannopoulos, D. Vanderbilt, R. J. Hamers, and J. E. Demuth, Phys. Rev. Lett. **64**, 2406 (1990).

[3] E. Pehlke and J. Tersoff, Phys. Rev. Lett. **67**, 465 (1991).

[4] E. Pehlke and J. Tersoff, Phys. Rev. Lett. **67**, 1290 (1991).

[5] For a given θ and ϵ, the elastic energy is minimized as a function of p, and the stiffness coefficient is the second-order coefficient at this minimum. $\kappa(\theta,\epsilon)=\pi^2\tan^2\theta[1+\tan^2(p\pi/2)][9.32-403.48\tan\theta\tan(p\pi/2)]$, where $\tan(p\pi/2)=0.0231/\tan\theta[1-\sqrt{1+1.05\epsilon-\tan^2\theta/0.000\,534}]$.

[6] When the SB steps fluctuate large enough to make contact with SA steps, the SL steps and the DL step are not distinguishable any more. The description of the surface structure based on separate Hamiltonians are no longer valid, and this breakdown is expected to occur within the temperature range $300<T<500$ K.

[7] O. L. Alerhand, D. Vanderbilt, R. D. Meade, and J. D. Joannopoulos, Phys. Rev. Lett. **61**, 1973 (1988).

[8] T. W. Poon, S. Yip, P. S. Ho, and F. F. Abraham, Phys. Rev. Lett. **65**, 2161 (1990).

[9] M. B. Webb, K. F. Men, B. S. Swartzentruber, R. Kariotis, and M. G. Lagally, Surf. Sci. **242**, 23 (1991).